Calculation of vibrational properties of selenium

1997 J. Phys.: Condens. Matter 9 1049

(http://iopscience.iop.org/0953-8984/9/5/011)

J. Phys.: Condens. Matter **9** (1997) 1049–1066. Printed in the UK PII: S0953-8984(97)78386-3

Calculation of vibrational properties of selenium

C Oligschleger† and J C Schön‡

† Institut für Algorithmen und Wissenschaftliches Rechnen, GMD, Forschungszentrum Informationstechnik, D-53754 St Augustin, Germany

‡ Institut für Anorganische Chemie und SFB408, Universität Bonn, Gerhard-Domagk-Strasse 1, D-53121 Bonn, Germany

Received 4 October 1996

Abstract. Using molecular dynamics with a classical interaction potential we present methods for calculating both vibrational properties and thermodynamic quantities for solids and estimating their temperature dependence. The density of states is given by the Fourier transformation of the displacement autocorrelation function. Applying the harmonic approximation we calculate the specific heat c_v. Elastic constants are determined from the response of the structures to external pressures and volume changes. As an example, crystalline and amorphous modifications of selenium are considered.

1. Introduction

One of the central goals in physics, chemistry, and technology is the description and prediction of properties of real molecules and condensed systems.

A crucial property of solids is their vibrational density of states (DOS) that can be measured experimentally with inelastic neutron, infrared (IR) and Raman scattering, since many thermodynamic properties, e.g. the specific heat c_v, depend on the vibrational spectrum. Furthermore, the low-frequency behaviour of the phonons is correlated with the elastic properties of the solid, whereas the high-frequency optical modes typically reflect the interactions between nearest or next-nearest neighbours. Therefore, a theoretical investigation and simulation of the DOS can provide insight into both macroscopic properties of the solid, e.g. elastic constants, and the microscopic dynamics of the atoms [1].

Numerical calculations of the vibrational DOS, e.g. using Born–von Kármán models, are often based on the harmonic approximation of the energy, where the anharmonic terms of the interaction potential are neglected. Here, we will present a method similar to the one proposed by Beeman and Alben [2] to calculate the vibrational spectrum. In their original paper, Beeman and Alben developed an algorithm for calculating the density of states by solving the equation of motion (EOM), where the forces are given in the harmonic approximation. The density of states is obtained by the Fourier transformation of the displacement autocorrelation function observed over a sufficiently long time interval. The EOM method suffers from the finite resolution of the frequencies and the lack of information about eigenmodes of the structures, however.

Another method applied successfully to condensed matter in order to obtain the DOS is the velocity-autocorrelation function [3, 4]. This method can be used effectively in the simulation of liquids [5], where the velocity-autocorrelation function is also a measure for the diffusion of the atoms.

0953-8984/97/051049+18$19.50

To determine the influence of anharmonic effects we have applied this method employing the full interaction potential. This enables us to study the temperature dependence of vibrational and thermodynamic properties of solids. From the density of states we can derive the specific heat c_v in the harmonic approximation [6]. Using constant-temperature and constant-pressure molecular dynamics, we can also compute volume changes of the structures, which allow us to calculate the thermal expansion coefficient. These volume changes are connected with a change in the vibrational spectrum, leading in many systems to a softening of modes. This observation is expressed in quantitative terms by the Grüneisen parameter.

However, due to finite-size effects ($L_{\mathrm{cell}} < \infty$), which place a lower bound on the possible $\boldsymbol{k}$-vectors ($|\boldsymbol{k}| \geqslant 2\pi/L_{\mathrm{cell}}$), one cannot determine the elastic constants of the structures from the vibrational density of states. Instead, we will estimate the elastic constants and sound velocities by computing the response of the simulated structures to applied stresses/strains.

A much more direct approach to the problem of determining eigenfrequencies and the corresponding eigenmodes is the diagonalization of the dynamical matrix of the system. Given a three-dimensional configuration with N atoms and an analytic interaction potential, one can calculate the matrix of second derivatives of the potential energy with respect to the positions of the atoms. Thus, diagonalization of this $3N \times 3N$ matrix yields $3N$ eigenvalues and eigenvectors. Although for large sparse systems there exist methods [7] for quickly determining at least the lowest eigenvalues of the spectrum, the number of atoms which can be simulated is often restricted due to storage limitations. From a physical point of view, however, a much more important shortcoming of relying on the diagonalization of the dynamical matrix is the total neglect of anharmonic terms in the potential.

In order to test and compare these two approaches, we have applied the corresponding algorithms to structures of selenium (both crystalline and glassy configurations) generated with a classical interaction potential [8].

In the next section, we describe the system which we have used as a test case for the algorithms, and the corresponding interaction potential. In section 3, we explain the methods in detail. The results are presented in section 4. Finally, we discuss our results, and compare with experiments.

2. Example system

Selenium readily forms glasses and amorphous structures [9]. There exist several crystalline structures, including two (α- and β-) monoclinic forms with four eight-membered rings packed differently in the unit cell. The most stable crystalline phase under standard conditions consists of infinite helical chains with trigonal symmetry [9, 10].

The potential that we have used was taken from the literature [8]. The parametrization of the potential was chosen to mimic certain structural properties of selenium: the potential was fitted to reproduce bond lengths, angles and bonding energies of small Se molecules [11], and gives a reasonable description of the trigonal crystal [10, 12, 13].

In the following we give a short description of the potential that resembles the one proposed by Stillinger *et al* to model sulphur [14]. The covalent bonds between Se atoms are modelled using short-range interactions. The effective interatomic potential U is strongly

repulsive for small interatomic distances and includes two- and three-body interactions†:

$$U = \sum_{i<j} V_2(r_{ij}) + \sum_{i<j<k} h(r_{ij}, r_{kj}, \Theta_{ijk}) + \text{cyclic permutations} \tag{1}$$

where $V_2(r_{ij})$ is the two-body contribution of the potential energy U for atoms i and j separated by distance r_{ij}. The three-body interaction depends on r_{ij}, r_{jk}, and Θ_{ijk}, the angle at atom j subtended by $\boldsymbol{r}_{ij}$ and $\boldsymbol{r}_{jk}$. The three-particle energy $h(r_{ij}, r_{jk}, \Theta_{ijk})$ is given by

$$h(r_{ij}, r_{jk}, \Theta_{ijk}) = V_3(r_{ij})V_3(r_{jk})(b_1(\cos\Theta_{ijk} - \cos\beta_2)^2 + b_3 - 0.5b_1\cos^4\Theta_{ijk}) \tag{2}$$

with $b_1 = 34.4866$, $b_3 = 11.9572$ and $\beta_2 = 95.3688^\circ$. The three-body term is purely repulsive and strongly favours the coordination number two as observed in experiment. The angular dependence reflects the preference for θ-values of $\approx 100^\circ$. The $\cos^4$ term was introduced in order to stabilize the Se chains of the trigonal phase against torsional displacements relative to each other.

To simplify the numerical calculations, the radial parts of the two- and three-body potentials of equations (1) and (2) are described by decaying exponential functions. Discontinuities in the vibrational frequencies are avoided by cutting off the potentials smoothly as polynomials to yield continuous functions with continuous first and second derivatives at the cut-off distances:

$$V_{2,3}(r) = \begin{cases} a_{2,3}\exp(\alpha r) + b_{2,3}\exp(\beta r) + c_{2,3}\exp(\gamma r) & r < 1.6 \\ d_{2,3}(r - r_{2,3})^5 + e_{2,3}(r - r_{2,3})^4 + f_{2,3}(r - r_{2,3})^3 & 1.6 < r < r_{2,3} \\ 0 & r > r_{2,3}. \end{cases} \tag{3}$$

Table 1. Parameters for the two- and three-body potentials (in r.u.) (from reference [8]).

	Two-body potential	Three-body potential
	$r < 1.6$	$r < 1.6$
a	928.12	8.8297
b	0.268 02	−2.5932
c	−16.599	−6.9384
α	−7.984	−0.476 01
β	−0.000 077 781	−1.5637
γ	−1.8634	−0.370 49
	$1.6 < r < 2.37$	$1.6 < r < 2.35$
d	1.868 25	0.225 56
e	4.586 28	0.125 27
f	3.620 29	−0.210 19
$r_{2,3}$	2.37	2.35

The exponential part of the interaction potential includes the nearest-neighbour shell (1.6 r.u. = 2.79 Å), while the long-range behaviour is described by the cut-off function. The cut-off distances are denoted by $r_{2,3}$ for the two- and three-body potentials, respectively. The corresponding parameters are listed in table 1.

† We use 'reduced' units (r.u.) based on the experimental bond length (1.337 r.u. = 2.34 Å) and dissociation energy (0.697 r.u. = 2.24 eV) of the Se_8 molecule.

3. Methods and calculations

Molecular dynamics (MD) enables us to investigate structural, dynamical and thermodynamic properties of complex systems [1, 5, 15]. Using MD methods, one can simulate the time evolution of interacting particles and determine their dynamics by solving the equation of motion (EOM):

$$m_i \ddot{\boldsymbol{r}}_i = \boldsymbol{F}_i = -\sum_j \frac{\partial U}{\partial r_{ij}}. \tag{4}$$

Here, m_i is the mass of atom i, $\ddot{\boldsymbol{r}}_i$ is the acceleration and $\boldsymbol{F}_i$ the force on particle i, which is the derivative of the total potential energy U with respect to the coordinates of the atoms.

This numerical integration of Newton's equation of motion is performed with a discrete time-step $\tau \ll t_{\min}$, where $t_{\min}$ is the inverse of the largest vibrational frequency of the system. We use the velocity Verlet algorithm [16] to integrate the EOM with time-steps $\tau < 3.88$ fs and smaller.

To avoid or at least to reduce surface effects, we apply periodic boundary conditions. We simulate either microcanonical (N, V, E) or isobar/isothermal (N, p, T) ensembles. The pressure is calculated using a method proposed by Nosé and Klein [17]. The temperature of the system is computed from the equipartition theorem, and is given by

$$k_B T = \frac{1}{3N} \sum_{i\alpha} m_i \langle v_{i\alpha}^2 \rangle \tag{5}$$

where k_B is the Boltzmann constant.

Due to the use of the short-range interaction potential described in the previous section, we are able to reduce the amount of numerical calculations through the use of neighbour lists.

3.1. The density of states

To investigate the vibrational properties of solids with numerical methods, one has to keep in mind that computer storage and CPU time limit the number of atoms which can be simulated. Using classical methods like MD, the accessible number of particles representing the solid ranges from several hundreds of atoms upward to several thousands of particles. Therefore, modes with long wavelengths (like sound waves) which are always present in solids cannot be described by such confined, small structures with side-lengths of the order of typically only ten nearest-neighbour distances. Thus, the system size defines the shortest possible $\boldsymbol{k}$-vector and leads to finite-size effects.

For the simulation of the vibrational DOS, we use an algorithm proposed by Beeman and Alben [2]. In this algorithm the EOM is solved numerically by setting all velocities of the particles at $t = 0$ equal to zero, and the initial displacements of the atoms are set to

$$x_{i\alpha}(t = 0) = x_{i\alpha}^0 \tag{6}$$

with

$$\begin{aligned} x_{i\alpha}^0 &= \sqrt{2}(\cos\Theta_{i\alpha})q \\ A_{i\alpha}^0 &= \sqrt{2}(\cos\Theta_{i\alpha})/q \end{aligned} \tag{7}$$

where i denotes the atoms and α the Cartesian directions. The angles $\Theta_{i\alpha}$ are distributed randomly between 0 and 2π, and the magnitude of the displacements is scaled by q and determines the temperature of the samples.

The DOS $Z(\omega)$ is given by

$$Z(\omega) = \left\langle \frac{2}{\pi} \int_0^{t_{\rm obs}} \sum_{i,\alpha} A^0_{i\alpha} x_{i\alpha}(t) (\cos(\omega t)) \exp(-\lambda t^2)\ {\rm d}t \right\rangle \tag{8}$$

where $\langle \cdots \rangle$ denotes the ensemble average. The choice of random angles $\Theta_{i\alpha}$ in the initial conditions for the atomic displacements $A^0_{i\alpha}$ and $x^0_{j\beta}$ has the advantage that for the average of products of random cosines we find

$$\frac{2}{\pi} \langle \cos(\Theta_{i\alpha}) \cos(\Theta_{j\beta}) \rangle = \delta_{ij} \delta_{\alpha\beta}. \tag{9}$$

Using a non-zero value of λ, the exponential factor in equation (8) leads to a broadening of the δ-peaks in the frequency spectrum.

In the harmonic approximation, which had been employed in the EOM procedure by Beeman and Alben [2], one can decompose the random, initial displacements as well as the atomic displacements at time t into the eigenvectors of the system:

$$x_{i\alpha}(t) = \frac{1}{\sqrt{m_i}} \sum_n U_n(i\alpha) c_n \cos(\omega_n t) \tag{10}$$

where $U_n(i\alpha)$ is the component of atom i in direction α of the nth normal mode of the system considered, c_n are the expansion coefficients (amplitudes) of these vibrations and ω_n is the corresponding frequency of the nth eigenmode. In particular, one can write a similar equation for the initial conditions; and one finds an expression for the amplitudes c_n:

$$c_n = \sum_{j\beta} U_n(j\beta) x^0_{j\beta} \sqrt{m_j}. \tag{11}$$

Then, the density of states can be written as

$$Z(\omega) = \left\langle \frac{2}{\pi} \int_0^{t_{\rm obs}} \sum_{i,\alpha} \sum_{j,\beta} \sum_n \sqrt{\frac{m_j}{m_i}} U_n(i\alpha) U_n(j\beta) A^0_{i\alpha} x^0_{j\beta} \cos(\omega_n t) \cos(\omega t) \exp(-\lambda t^2)\ {\rm d}t \right\rangle. \tag{12}$$

Rewriting the product of the cosines as a sum leads to

$$Z(\omega) = \left\langle \frac{1}{\pi} \int_0^{t_{\rm obs}} \sum_{i,\alpha} \sum_{j,\beta} \sum_n \sqrt{\frac{m_j}{m_i}} U_n(i\alpha) U_n(j\beta) \times A^0_{i\alpha} x^0_{j\beta} (\cos((\omega + \omega_n)t) + \cos((\omega - \omega_n)t)) \exp(-\lambda t^2)\ {\rm d}t \right\rangle. \tag{13}$$

Due to the frequency–time uncertainty principle, the spectral resolution $\Delta\omega$ is inversely proportional to the observation time $t_{\rm obs}$. As shown in the original paper [2], the finite integration time $t_{\rm obs}$ and a non-zero value of λ will give a Gaussian-like contribution for each mode, leading to a broadening of the vibrational spectrum.

It is only in the limits $t_{\rm obs} \to \infty$ and $\lambda \to 0^+$ that the integral

$$\frac{1}{\pi} \int_0^{t_{\rm obs}} \cos(xt) \exp(-\lambda t^2)\ {\rm d}t$$

will give a δ-peak for each vibrational state. Thus, the choice of the parameter λ and the finite observation time $t_{\rm obs}$ influences the resolution of the spectral density and the spectral broadening of the vibrational modes.

Obviously, in order to obtain the DOS with this procedure, one has to average over several (N_r) EOM runs. In order to estimate the quality of the resulting spectrum, we have investigated how the accuracy depends on the number of runs used in averaging, N_r.

The amplitude q of the initial random atomic displacements is intimately connected to the temperature of the system. The larger the amplitude, the higher the kinetic energy of the system, which essentially defines the temperature.

Since the applied effective model potential contains anharmonicities, we can study their influence on the spectral properties, which becomes more and more important at higher temperatures when the amplitudes of the atomic vibrations are no longer small. A very important consequence of the anharmonic potential is the phenomenon of thermal expansion of solids which cannot be explained by the harmonic approximation. Another important influence of anharmonicities is the finite lifetime of phonons which are no longer stationary states of the system. Thus, phonons will decay or merge into other ones. However, since this decay of the eigenmodes is rather slow, compared to many vibrational processes, one can continue to describe such phenomena, e.g. the specific heat, in terms of phonons. Typical lifetimes of phonons are of the order of 10–100 ps (or even longer), at temperatures well below the melting point [18]. In order to test the assumptions, we have prepared our system in a well defined state by excitation of eigenmodes and followed the dynamics. We observe that the single eigenmodes do not decay appreciably on a time-scale less than 40 ps. This time span is significantly longer than the time necessary to calculate the vibrational DOS (several ps). Thus, one can still interpret the DOS computed using equation (8) as the DOS of $3N$ (harmonic) phonons, with possibly shifted frequencies.

As was pointed out in the introduction, a direct way to calculate the vibrational spectrum is to diagonalize the dynamical matrix $\mathbf{D}$, whose elements are

$$D_{ij}^{\alpha\beta} = \frac{1}{\sqrt{m_i m_j}} \frac{\partial^2 U}{\partial R_i^\alpha \partial R_j^\beta}. \tag{14}$$

Here U is the total potential energy (equation (1)), the derivatives are with respect to the positions $\boldsymbol{R}_i$ and $\boldsymbol{R}_j$ of atoms i and j, and α and β stand for the Cartesian directions. m_i and m_j are the atomic masses. For a block containing N atoms one has to diagonalize a $3N \times 3N$ matrix, whose eigenvalues are the squares ($\omega_\sigma^2 = (2\pi\nu_\sigma)^2$) of the vibrational mode frequencies. The diagonalization can be solved with standard routines, e.g. EISPACK, which use factorization methods to diagonalize matrices [19]. The great advantage of this direct method is that it allows us to calculate all the eigenfrequencies and eigenmodes of the structure. Comparing the results of this direct method with the spectrum computed using the EOM method, we can judge the quality of the latter technique.

3.2. Elastic constants

As was mentioned in the previous section, the finite system sizes lead to a cut-off at the low-frequency end of the vibrational spectrum.

This systematic lack of information about acoustic modes can be partly alleviated by calculating the sound velocities, which determine the Debye spectrum

$$Z_D(\nu) = \frac{3}{\nu_D^3}\nu^2 \tag{15}$$

from the elastic constants. In equation (15),

$$\nu_D = \bar{c}\left(\frac{3\rho}{4\pi m}\right)^{1/3} \tag{16}$$

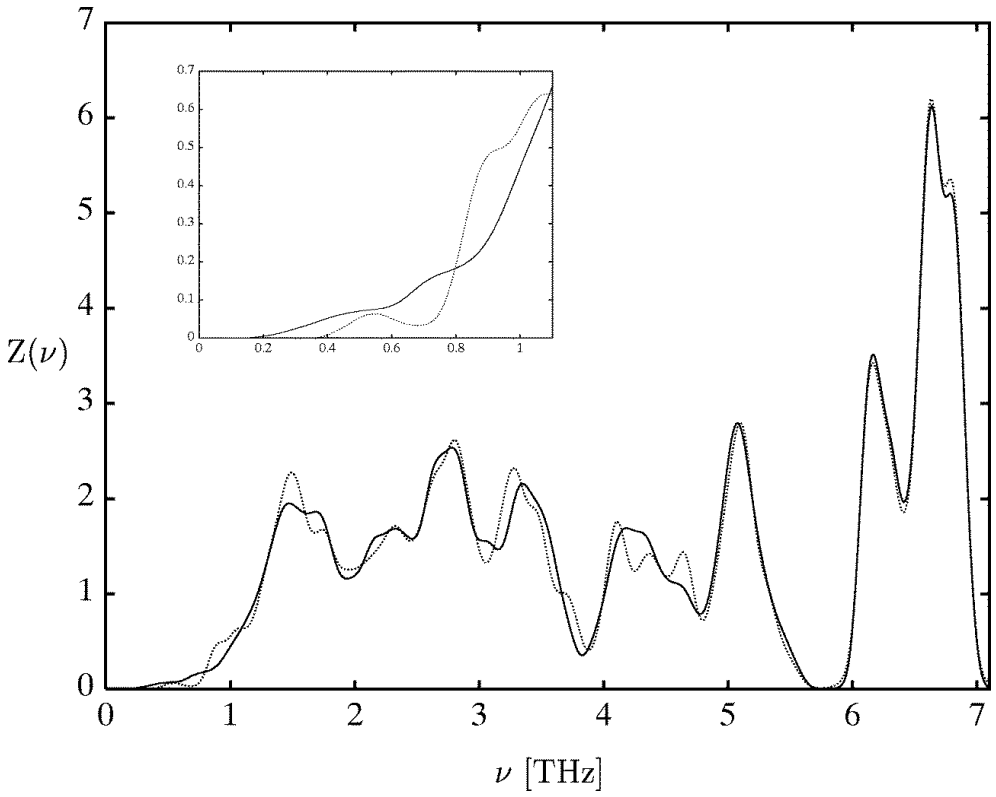

Figure 1. The vibrational density of states Z as a function of the frequency ν (THz) for a trigonal Se crystallite with 1470 atoms/cell (the dotted line) and with 11 760 atoms/cell (the solid line), respectively. Both spectra are averaged over 10 different sets of initial conditions, with a displacement amplitude $q = 0.001$ ($T \approx 0.2$ K) and an observation time $t_{\mathrm{obs}} = 1800$ MDS. The inset shows the low-frequency range of these spectra: solid line: the spectrum for the system with $N = 11\,760$ atoms; dotted line: the spectrum for the system with $N = 1470$ atoms. One can clearly see the system size effect on the lowest possible frequency.

where $\bar{c}$ is the average sound velocity, and ρ is the density of the structure considered. The—in the case of trigonal Se, anisotropic—sound velocities are directly connected to the elastic constants:

$$v_{ij} = \sqrt{c_{ij}/\rho}. \tag{17}$$

We calculate the elastic constants of the structure from the change in potential energy, ΔE_{pot}:

$$\Delta E_{pot} = -\sum_{\alpha\beta} P_{\alpha\beta}\epsilon_{\alpha\beta} + \frac{V}{2}\sum_{\alpha\beta\gamma\delta}\epsilon_{\alpha\beta}C_{\alpha\beta\gamma\delta}\epsilon_{\gamma\delta} + \frac{1}{2}\sum_{\alpha\beta\gamma} P_{\alpha\beta}\epsilon_{\alpha\gamma}\epsilon_{\gamma\beta} \tag{18}$$

due to an applied strain

$$R_\alpha^m \rightarrow R_\alpha^m + \sum_\beta \epsilon_{\alpha\beta}R_\beta^m. \tag{19}$$

Here R_α^m is the coordinate of atom m in direction $\boldsymbol{\alpha}$ and $\boldsymbol{\epsilon}$ is a transformation matrix, which determines the shape of the system cell and the relative dilatation/compression of the structure.

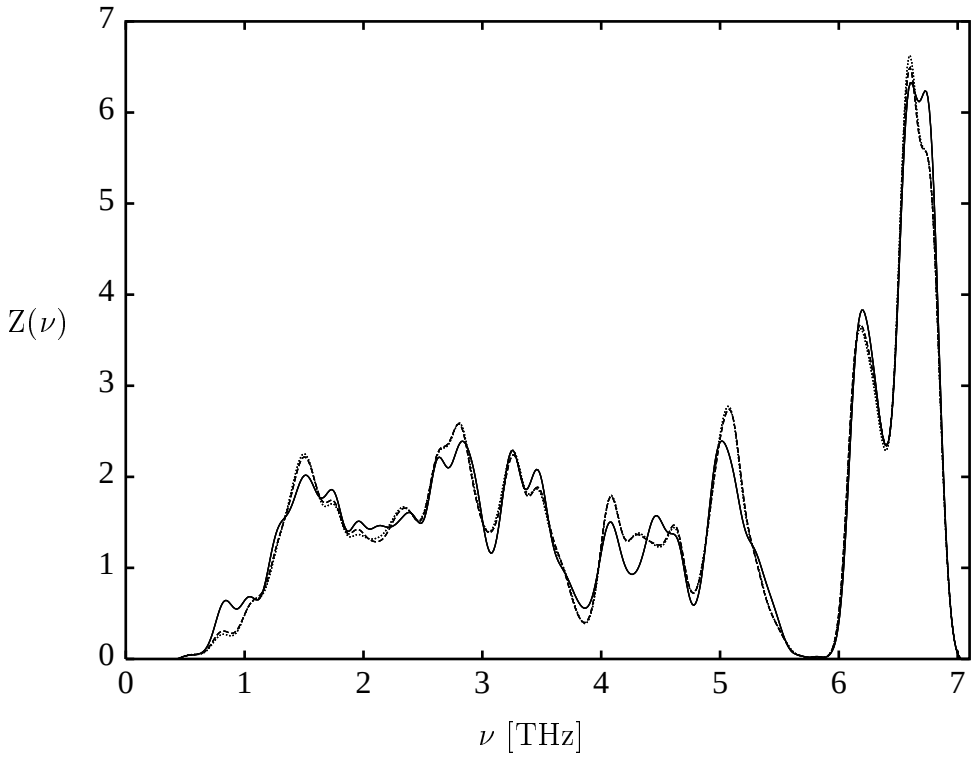

Figure 2. The vibrational density of states Z as a function of the frequency ν (THz) for a trigonal Se crystallite with 1470 atoms/cell. We present the result for one set of initial conditions (the solid line), together with the results obtained by averaging over 10 sets (the dashed line) and 20 sets (the dotted line). The damping factor is $\lambda = 4/t_{\mathrm{obs}}^2$.

The first term in equation (18) accounts for the work done against all of the forces for a system which was not prepared in a configuration in equilibrium with respect to volume changes. $P_{\alpha\beta}$ is the virial of the forces. The third term, present for shears only, is a correction for the volume change under a finite shear, and the $C_{\alpha\beta\gamma\delta}$ are the elastic constants (in the Voigt notation one has e.g. $c_{11} = C_{1111}$, $c_{44} = C_{2323}$ [20]).

For symmetry reasons, trigonal Se possesses six independent elastic constants: $c_{11,33,44} \leftrightarrow v_{11,33,44}$—longitudinal; $c_{66,13,14} \leftrightarrow v_{66,13,14}$—transverse; $c_{12} = c_{11} - 2c_{66} \leftrightarrow v_{12}$—transverse.

Applying appropriate stresses and strains one can determine the energy changes of the system and, using equation (18), one can calculate the corresponding elastic constants.

We use constant-volume MD, in order to measure the internal pressures in the system that appear as response to a volume change initially applied (cf. equation (19)). The resulting internal pressures are a measure of the product of the volume expansion coefficient κ and the bulk compression $\tilde{K}$. Furthermore, we also perform constant-pressure simulations to calculate the resulting volume changes of the configurations. These volume changes can be used to determine the thermal expansion coefficient κ. The advantage of utilizing MD instead of static methods lies in the possibility of estimating the temperature dependence of the elastic constants.

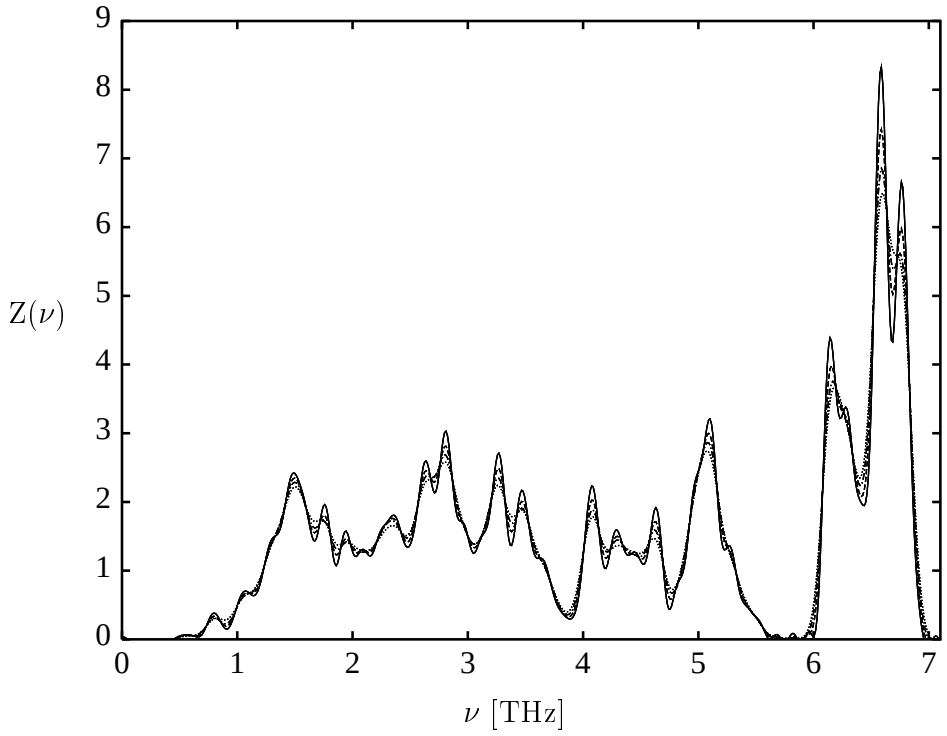

Figure 3. The vibrational DOS Z versus the frequency ν (THz) for a trigonal Se crystallite with 1470 atoms/cell, for different damping factors: $\lambda = 1/t_{obs}^2$ (the solid line), $\lambda = 2/t_{obs}^2$ (the dashed line), $\lambda = 3/t_{obs}^2$ (the chain line) and $\lambda = 4/t_{obs}^2$ (the dotted line).

4. Results

4.1. The vibrational density of states

In the following we will investigate systematically the influence of the parameters listed in subsection 3.1 on the DOS.

4.1.1. The system size and finite-size effects. To investigate system size effects we study structures consisting of $N = 1470$ and 11 760 atoms in the simulation cell. In figure 1, we show the resulting densities of states for trigonal crystals comprising $N = 1470$ (the dashed line) and $N = 11\,760$ atoms (the full line), respectively. To calculate the vibrational spectra, the EOM of these structures are integrated for a time interval $t_{obs} = 1800$ MDS (which corresponds to approximately 3.88 fs). We use ten sets of initial conditions with an amplitude $q = 0.001$ (which corresponds to a temperature $T \approx 0.2$ K). The damping factor λ is set to $4/t_{obs}^2$.

The overall features, e.g. the positions of the peaks and the shape of the vibrational spectra, are very similar for the two system sizes. However, as shown in the inset, the lowest frequency scales approximately with the system size. This result follows from the fact that doubling the linear dimensions of the structure halves the frequency of the phonons that can exist in solids limited in system size.

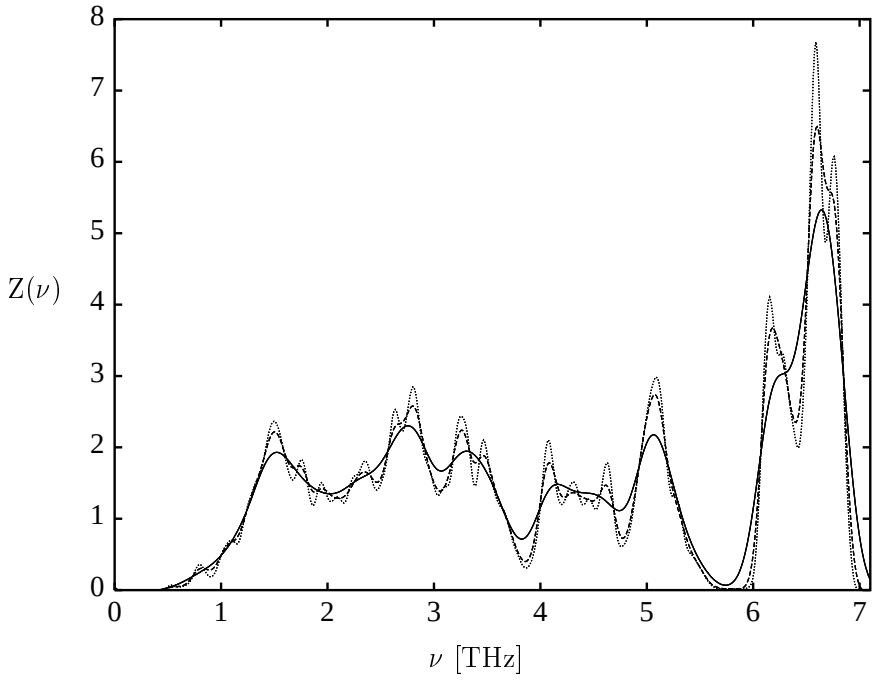

Figure 4. The vibrational density of states Z as a function of the frequency ν (THz) for a trigonal Se crystallite with 1470 atoms/cell, for different observation times: $t_{\mathrm{obs}} = 900$ MDS (the solid line), $t_{\mathrm{obs}} = 1800$ MDS (the dashed line) and $t_{\mathrm{obs}} = 2700$ MDS (the dotted line).

4.1.2. The number of sets, N_r, used for the averaging procedure. To obtain a good approximation of the vibrational spectrum with this procedure, one has to average over several sets of initial atomic displacements to improve the accuracy of the spectrum. We determine the displacement autocorrelation for a trigonal crystal with 1470 atoms; the amplitude of the atomic displacements is $q = 0.01$. The trajectories are followed over an observation time of 1800 MDS. The damping factor was chosen as $\lambda = 4/t_{\mathrm{obs}}^2$. Figure 2 shows the spectrum for a single set of initial conditions (solid line). Averaging over 10 different sets of initial displacements yields a more accurate spectrum (the dashed line). For comparison, we also show in figure 2 the resulting DOS calculated on the basis of 20 sets of random atomic displacements (the dotted line).

The difference between the spectrum with just one set of initial displacements and the other two is striking. Most of the structures and peaks present in the spectrum of a single EOM run vanish once we average over several sets. But the spectrum with just one set already exhibits properties of the typical DOS nevertheless.

The difference between the averaging over 10 different sets of initial displacements and 20 sets is practically negligible. Thus, using 10 sets appears to be sufficient to obtain reliable results in the case of selenium.

4.1.3. The influence of the damping factor λ and finite observation time t_{obs} on the spectral broadening. The effect of the choice of the damping factor λ is investigated for a crystal with $N = 1470$ atoms, a displacement amplitude $q = 0.01$, 10 sets of different initial conditions and an observation time $t_{\mathrm{obs}} = 1800$ MDS. In figure 3 we plot the result for

$\lambda = 1/t_{obs}^2$ (the solid line), for $\lambda = 2/t_{obs}^2$ (the dashed line), for $\lambda = 3/t_{obs}^2$ (the chain line), and for $\lambda = 4/t_{obs}^2$ (the dotted line), respectively.

The resolution of the frequency spectra increases with decreasing damping factor λ, and more and more details of the DOS of the finite-sized system become visible.

As mentioned in subsection 3.1, the integration time t_{obs} determines the spectral resolution of the calculated vibrational DOS. To clarify this point, we have performed MD runs with different observation times.

In figure 4 we plot the resulting spectra obtained for different integration times t_{obs} with damping factors $\lambda = 4/t_{obs}^2$. In all cases, the trigonal crystallite consists of $N = 1470$ atoms, and the amplitude of the initial displacements is set to $q = 0.01$. In all simulations, 10 different sets of initial conditions are used for the calculations of the average spectral densities. In figure 4 we show the vibrational spectrum obtained using the integration times $t_{obs} = 900$ MDS (the solid line), $t_{obs} = 1800$ MDS (the dashed line) and $t_{obs} = 2700$ MDS (the dotted line), respectively.

Clearly, an increase of the observation time yields a higher spectral resolution of the DOS in agreement with the uncertainty relation, and details of the structure of the underlying vibrational spectrum become more visible.

4.1.4. The correlation between the amplitude q and the temperature. The amplitude of the initial random atomic displacements influences the total energy of the system. The larger the amplitude of the atoms, the higher the total energy of the system, which is equally distributed between the potential energy and the kinetic energy (temperature), due to the equipartition theorem.

If the atoms are displaced far enough from their equilibrium positions, they can 'feel' the anharmonicity of the interaction potential. To study the influence of this anharmonicity, we perform MD runs with different amplitudes of the initial random displacements. We simulate a trigonal crystal under zero pressure and temperatures ranging from about 0.2 K to 180 K. In figure 5 the resulting spectrum of a crystal with temperature $T \approx 0.2$ K ($q = 0.001$; the solid line) is plotted; we also give the spectra for calculations performed at $T \approx 90$ K and 180 K, with $q = 0.025$ (the dashed line) and 0.035 (the dotted line), respectively.

At the high-frequency end, we observe a shift in the spectrum towards lower frequency with increasing temperature. Furthermore, the volume of the crystallite grows with increasing temperature. The shift in the frequency spectrum connected with volume change of the structures can be expressed by the Grüneisen parameter γ:

$$\gamma_i = -\frac{\partial \ln \omega_i}{\partial \ln V}$$
$$\gamma = \sum_i c_{vi}\gamma_i \Big/ \sum_i c_{vi} \tag{20}$$

where γ_i is the partial Grüneisen parameter of mode i and c_{vi} is the contribution of mode i to the specific heat c_v. From our spectra we determine a Grüneisen parameter $\gamma = 1.5$ that deviates from the values found experimentally by Grosse *et al* who report the Grüneisen parameter $\gamma = 1.9$–0.9 for $T = 10$–300 K [21].

The deviation of our theoretical value from the one observed in experiment can be explained by the insufficient description of the temperature dependence of the frequency spectrum, caused by the imperfect interaction potential.

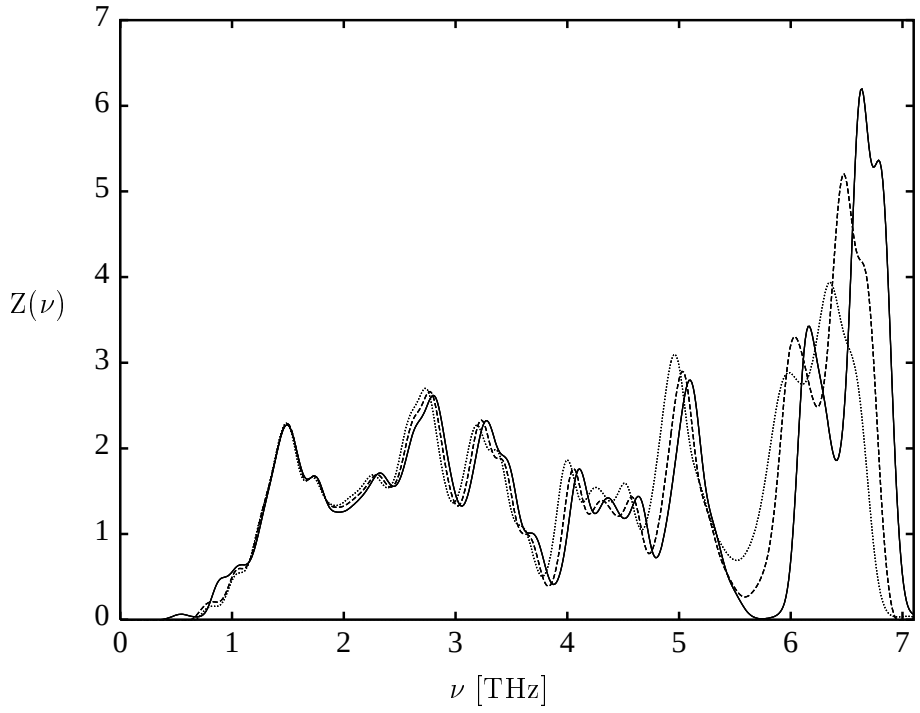

Figure 5. The vibrational density of states Z as a function of the frequency ν (THz) for a trigonal Se crystallite with 1470 atoms/cell. The temperature of the system is $T \approx 0.2$ K (the solid line), $T \approx 90$ K (the dashed line), and $T \approx 180$ K (the dotted line), respectively.

4.1.5. Comparison of the EOM method and the direct diagonalization. Figure 6 (the solid line) shows the density of states $Z(\nu)$ calculated for a crystallite of 1470 Se atoms at $T = 0$ K, using matrix diagonalization.

The spectrum of the 4410 eigenfrequencies of the trigonal structure is plotted using bins on the frequency axis with a bin width $\Delta\nu = 0.103$ THz. Comparing the exact spectrum with a DOS obtained from EOM runs (the dashed line), which corresponds to the spectrum at temperature $T \approx 0.2$ K, the lowest temperature that we have used in our simulations), we find a satisfactory agreement between the two spectra. The location of the main peaks of the DOS is identical in the two cases. There exist some deviations in the location of shoulders, which might be due to the choice of the bins used in plotting the spectrum in figure 6. We note that the calculation of the vibrational DOS using the EOM method yields a smooth and continuous spectrum, due to the finite resolution in the frequency range. In contrast, employing direct diagonalization methods, the resulting spectra were rugged because the small systems that can be treated with these techniques possess discrete eigenvalues. Of course, the spectrum becomes more dense when the size of the system is increased. Nevertheless, the main advantage of diagonalization methods is the possibility of determining (in the harmonic approximation) the eigenvalues and eigenvectors of the structures explicitly.

4.1.6. Comparison of the calculated crystalline (optimal) spectrum with experiment. The reliability of the potential employed can be checked by comparing the calculated results with

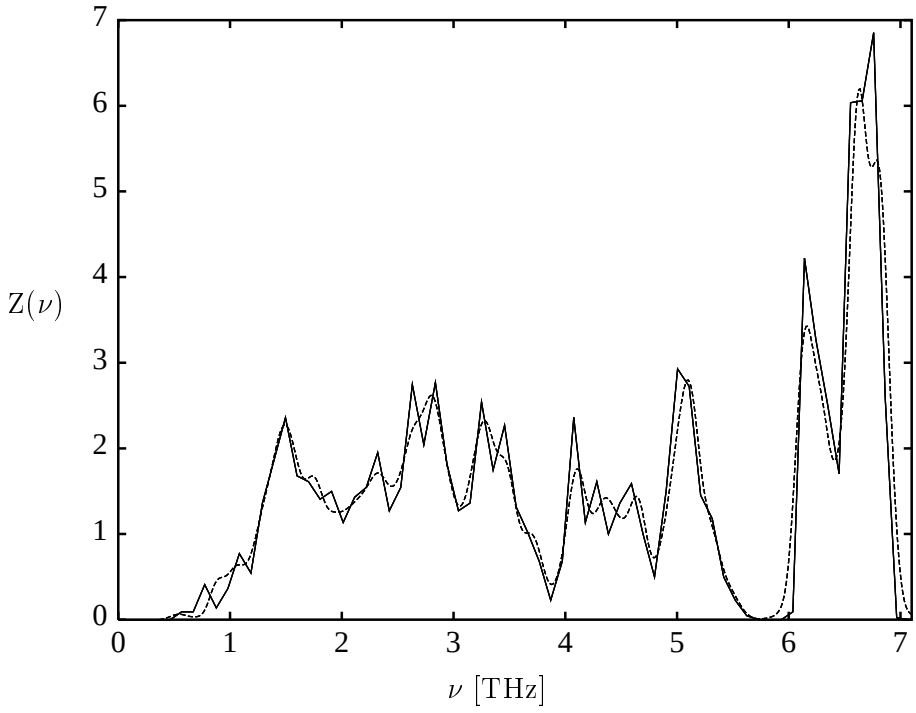

Figure 6. The vibrational density of states Z as a function of the frequency ν (THz) for a trigonal Se crystallite with 1470 atoms/cell. The spectrum is derived by diagonalizing the dynamic matrix **D** [8].

experiments. The agreement is mostly satisfactory, although the vibrational DOS measured by Gompf [22] reveals a higher density at the low-frequency end of the spectrum than we find in our model. Also, the gap separating the middle part of the spectrum from the high-frequency modes is too small, and the highest frequencies are too low, compared with experimental findings [23, 24].

4.1.7. Glasses. In order to extend our simulation to other, non-crystalline structures we have performed simulations of the vibrational spectrum of Se glass. Using the EOM method we average over 10 different Se glasses found in previous simulations [25]. The structures comprise 1470 atoms. As parameters for the EOM runs, we employ $q = 0.002$, $N_r = 10$, $t_{\mathrm{obs}} = 2700$ MDS, and $\lambda = 4/t_{\mathrm{obs}}^2$. Figure 7 shows the calculated vibrational DOS of Se glass. In contrast to the spectrum of the trigonal phase, we do not find a pronounced gap in the spectrum. But, nevertheless, we observe a high-frequency peak typical for selenium. Some details of the spectrum for $\nu < 5$ THz that are reported by Bondybey and English [26] are not reproduced by our results; in particular, the peak positions of the librational and torsional modes are not separated. These deviations from experiment are due to the interaction potential that we have employed in our calculations. Since the spectrum is obtained at a temperature $T = 3.7$ K, we can compare the EOM result with a calculation based on the direct diagonalization of the dynamical matrix ($T = 0$ K). The differences are practically negligible. This result confirms the strength of the EOM algorithm as a method for determining spectral properties.

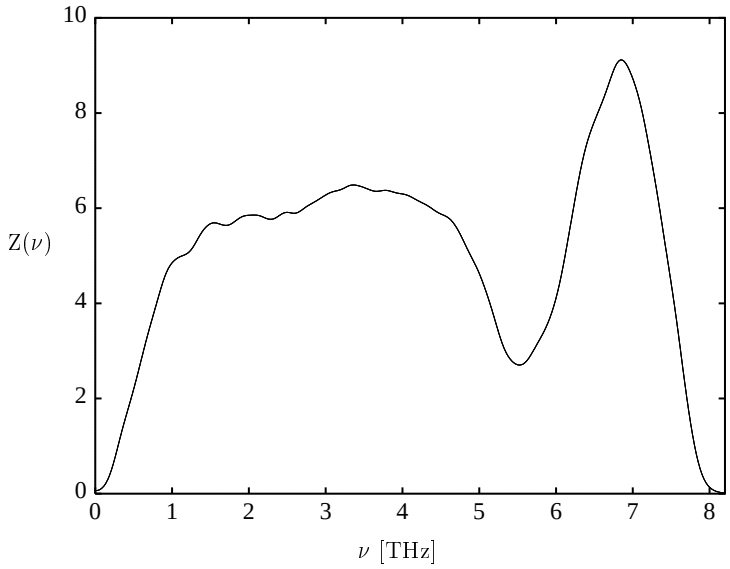

Figure 7. The vibrational density of states Z as a function of the frequency ν (THz) averaged over 10 Se glasses with 1470 atoms/cell each. The spectrum is obtained by employing the EOM algorithm.

Table 2. Elastic constants compared with experiments (reference [28]).

	Molecular dynamics			Experiments		
C_{ij} (GPa)	4 K	190 K	dC_{ij}/dT (10^7 Pa)	0 K	300 K	dC_{ij}/dT
C_{11}	122.3	122.8	0.25	25.0	16.7 to 19.0	−1.36 to −2.6
C_{33}	181.7	180.4	−0.68	91.0	74.1 to 105.0	−2.5 to 0.9
C_{44}	37.5	36.7	−0.48	24.0	12.5 to 18.2	−2.2 to 0.0
C_{66}	25.3	24.6	−0.37	10.0	5.8 to 8.0	−0.95 to −0.62
C_{12}	71.7	73.6	1.00	5.0	7.0	0.67
C_{13}	98.8	100.6	0.98	23.0	18.4	−1.3
C_{14}	−14.53	−14.52	0.004	−9.0	−7.6 to −5.0	1.0

4.2. Elastic constants

In table 2 we show the elastic constants at different temperatures and give estimates of the temperature dependence. The numerical results are compared with experiment. The rather large discrepancies between our calculations and experiments can be explained by the insufficient description of the low-frequency modes and their influence on the dynamics of the system, and by the absence of the long-wavelength acoustic modes in our model. These results are not unexpected, since the spectrum of the modelled trigonal selenium has already shown that the low-frequency modes, which are important for the elasticity of a material, are not described satisfactorily using our model interaction potential. Similarly, the dependence on temperature is too weak, since the low-frequency modes in the model system are too high.

4.3. Thermodynamic properties

In the following, we will give results concerning some thermodynamic properties and estimate their temperature dependence.

4.3.1. Thermal expansion. From the temperature dependence of the volume, we calculate the thermal volume expansion coefficient κ:

$$\kappa = \frac{1}{V}\left(\frac{\partial V}{\partial T}\right)_p. \tag{21}$$

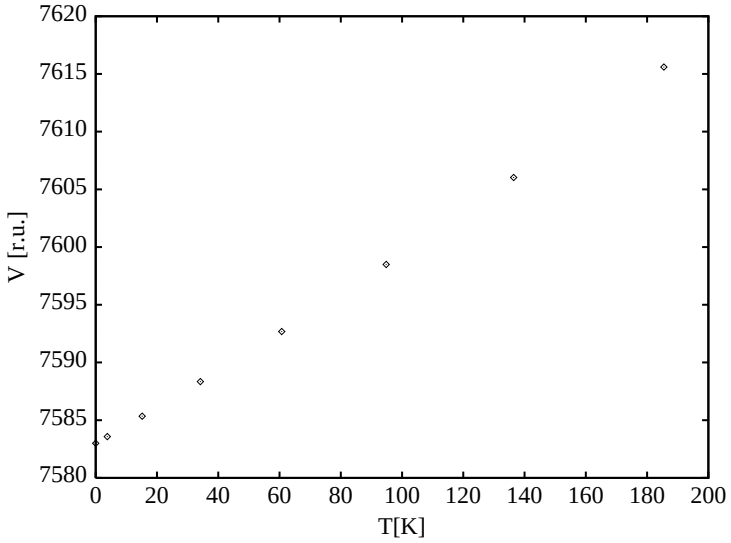

Figure 8. The volume V of the trigonal crystal plotted versus the temperature T.

In figure 8, we plot the volume V of the trigonal Se crystal averaged during constant-pressure/temperature MD runs versus the corresponding temperature T. The values of the thermal expansion coefficient κ range from 2.1×10^{-5} K^{-1} to 2.6×10^{-5} K^{-1} for $T = 0.2$–180 K. Experimentally the thermal expansion coefficient κ is found to be 0.3×10^{-5} K^{-1} to 12.6×10^{-5} K^{-1} for $T = 10$–300 K [21].

Furthermore, the determination of the internal average pressure p_{int} arising in MD runs at constant volume and temperature enables us to calculate the bulk compression $\tilde{K}$ via

$$\kappa\tilde{K} = \left(\frac{\partial p_{int}}{\partial T}\right)_V \tag{22}$$

where κ is the thermal volume expansion coefficient. From equation (22), we derive $\tilde{K} \approx 10.59 \times 10^{11}$ dyn cm^{-2}. Experimentally, $\tilde{K} = 1.74 \times 10^{11}$ dyn cm^{-2} has been reported [21].

4.3.2. The specific heat. From the vibrational DOS, we can determine the specific heat c_p in the harmonic approximation [27]:

$$c_p(T) = 3k_B \int \mathrm{d}\nu \left[\left(\frac{h\nu}{2k_BT}\right)^2 \Big/ \sinh^2(h\nu/2k_BT)\right] Z(\nu). \tag{23}$$

In the low-temperature limit the specific heat of a perfect crystal is proportional to T^3. But the low-temperature specific heat in glasses is typically an order of magnitude larger than in their crystalline counterparts due to the existence of additional low-frequency modes. In figures 9(a) and 9(b) we plot the specific heat as c_p/T^3 for both the Se glass and the trigonal crystal. Note that, because of the low-frequency modes missing in the simulated system, the calculated specific heat of the model is lower than that of 'real' selenium. Including the Debye contribution of the long-wavelength phonons, the difference between the calculation of the specific heat of the trigonal structure and the experimental values is reduced.

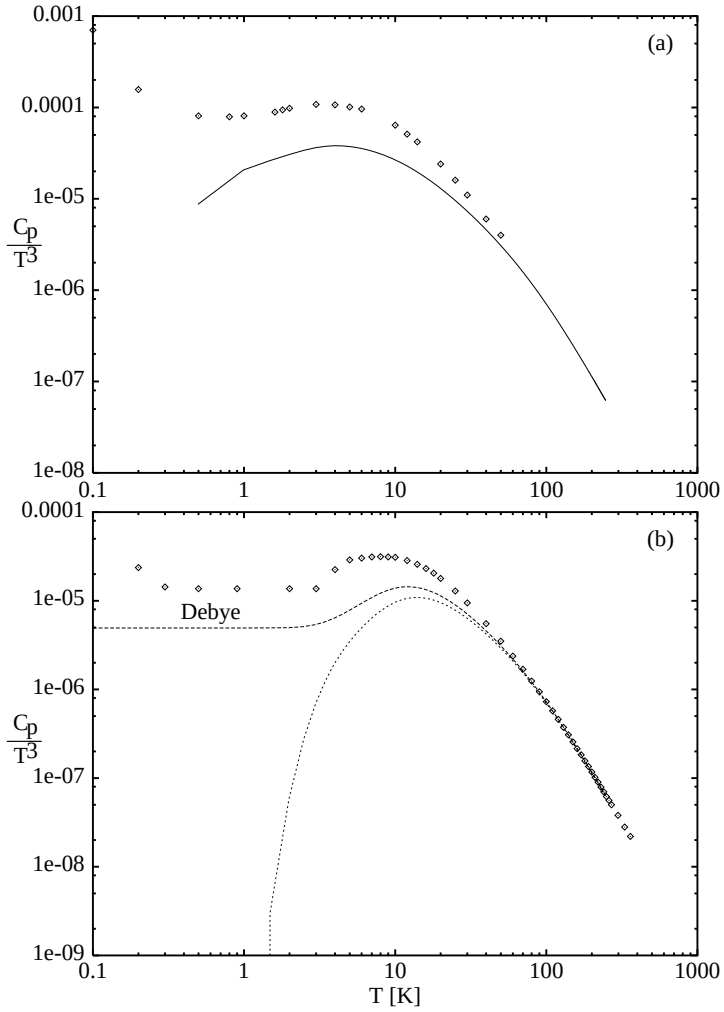

Figure 9. The specific heat c_p in units of $3k_B$ divided by T^3 plotted versus the temperature T in a double-logarithmic plot. (a) The full line shows the contribution of the spectrum of the glass plotted in figure 7. Diamonds show experimental data of Gaur *et al* [29]. (b) The dotted line shows the contribution of the spectrum of the trigonal crystal plotted in figure 5 (the solid line). The dashed line is the specific heat calculated for the spectrum with Debye correction. Diamonds show experimental data of Gaur *et al* [29].

5. Discussion and conclusions

Trying to calculate the DOS using MD is based on the fact that the vibrations of the atoms will dominate the dynamics of the atomic motions, and that vice versa the determination of the time evolution of the atomic displacements elucidates the vibrational spectrum.

As we have shown, one has to choose the parameters in the simulations (the number of atoms, number of different runs, displacement amplitude, observation time and damping factor) appropriately, in order to get a clear understanding of the vibrational DOS.

In addition, by applying stresses or volume changes, we can gain information about the elastic behaviour of the system. Since the elastic constants are directly connected to the sound velocities of a solid, their determination can at least alleviate the dearth of information concerning the low-frequency range of the DOS caused by the finite size of the systems modelled.

Quite generally, most problems encountered when applying these methods can be traced back to the finite size of the systems tractable using computers, leading to a lack of long-wavelength phonons in the simulations, and to the reliability of the interaction potential employed, especially with regard to the modelling of the soft modes.

These considerations also apply to our example, where the main shortcomings of the DOS and the thermodynamic properties computed are due to the lack of low-frequency acoustic modes. This also influences the simulation of the elastic behaviour of the trigonal crystal and of the amorphous structures of selenium. However, one should keep in mind that the potential had not been fitted to experimentally determined elastic constants, but instead to structural properties like bond lengths and bond angles of selenium.

To summarize, we have investigated the use of MD simulations to obtain information about vibrational and thermodynamic properties of solids. The great advantage of MD methods compared to direct diagonalization methods, when applied for calculating vibrational properties, lies in the possibility of gaining insight into anharmonic effects of solids if one can employ good anharmonic interaction potentials. Taking anharmonic effects into account, the algorithms presented are useful in determining the temperature dependence of thermodynamic quantities.

Acknowledgments

We gratefully acknowledge funding by the Deutsche Forschungsgemeinschaft through the Sonderforschungsbereich 408. This work has been conducted within the GMD research group ‘Computational Methods in Chemistry’ of the High-Performance Computing Centre (HLRZ). Parts of the calculations were performed on the IBM SP2 computer at the Institute for Algorithms and Scientific Computing (SCAI), German National Research Centre for Information Technology.

References

[1] Ciccotti G, Frenkel D and McDonald I R (ed) 1987 *Simulations of Liquids and Solids* (Amsterdam: North-Holland)
[2] Beeman D and Alben R 1977 *Adv. Phys.* **26** 339
[3] Dickey J H and Paskin A 1969 *Phys. Rev.* **128** 2589
[4] Klein M L 1986 Structure and dynamics of molecular crystals *Molecular-dynamics Simulations of Statistical-mechanics Systems* ed G Ciccotti and W G Hoover (Amsterdam: North-Holland)
[5] Allen M P and Tildesley D J 1987 *Computer Simulation of Liquids* (Oxford: Clarendon)
[6] Ashcroft N W and Mermin N D 1976 *Solid State Physics* (Saunders College, PA: HRW International Editions)

[7] *Harwell Subroutine Library* AERE Harwell, Didcot
[8] Oligschleger C, Jones R O, Reimann S M and Schober H R 1996 *Phys. Rev.* B **53** 6165
[9] Donohue J 1974 *The Structures of the Elements* (New York: Wiley) p 370
[10] Wyckoff R W G 1982 *Crystal Structures* (Malabar, FL: Krieger) p 36
[11] Hohl D and Jones R O 1991 *Phys. Rev.* B **43** 3856
[12] Hultgren R, Desai P D and Hawkins D T (ed) 1973 *Selected Values of the Thermodynamic Properties of the Elements* (Metals Park, OH: American Society for Metals)
[13] Mills K C 1974 *Thermodynamic Data for Inorganic Sulphides, Selenides and Tellurides* (London: Butterworths)
[14] Stillinger F H, Weber T A and La Violette R A 1986 *J. Chem. Phys.* **85** 6460
Stillinger F H and Weber T A 1987 *J. Phys. Chem.* **91** 4899
[15] Hansen J P and McDonald I R 1976 *Theory of Simple Liquids* (New York: Academic)
[16] Heermann D W 1990 *Computer Simulation Methods* (Berlin: Springer)
[17] Nosé S and Klein M L 1983 *Mol. Phys.* **50** 1055
[18] Schober H R and Petry W 1991 *Material Science and Technology* vol 1, ed R W Cahn, P Haasen and E J Kramer (Weinheim: VCH)
[19] Smith B T, Boyle J M, Dongarra J J, Garbow B S, Ikebe Y, Klema V C and Moler C B 1976 *Matrix Eigensystem Routines—EISPACK Guide* (Berlin: Springer)
[20] Voigt W 1889 *Ann. Phys., Lpz.* **33** 573
[21] Czack G, Kirschstein G and Kugler H K 1981 *Selen Gmelin Handbuch der Anorganischen Chemie* 8th edn, Ergänzungsband A3 (Berlin: Springer)
[22] Gompf F 1981 *J. Phys. Chem. Solids* **42** 539
[23] Teuchert W D, Geick R, Landwehr G, Wendel H and Weber W 1975 *J. Phys. C: Solid State Phys.* **8** 3725
[24] Bilz H and Kress W 1979 *Phonon Dispersion Relations in Insulators* (Berlin: Springer)
[25] Oligschleger C 1994 *PhD Thesis* (Reports of the Forschungszentrum Jülich: Report No 2968)
[26] Bondybey V E and English J H 1980 *J. Chem. Phys.* **72** 6479
[27] Born M and Huang K 1958 *Dynamical Theory of Crystal Lattices* (Oxford: Clarendon)
[28] Meißner M and Mimkes J 1979 *Physics of Selenium and Tellurium* ed E Gerlach and P Grosse (Berlin: Springer)
[29] Gaur U, Shu H-C, Mehta A and Wunderlich B 1981 *J. Phys. Chem. Ref. Data* **10** 89